IEEE Access
Multidisciplinary | Rapid Review | Open Access Journal

Received 12 September 2024, accepted 3 October 2024, date of publication 9 October 2024, date of current version 21 October 2024.

Digital Object Identifier 10.1109/ACCESS.2024.3477249

RESEARCH ARTICLE

Performance Analysis of the Underactuated Finger for Adam's Hand

ANDREA GRAZIOSO[1,2], DAMIANO COSMA POTENZA[1,2], GIOVANNI ANTONIO ZAPPATORE[2], AND GIULIO REINA[1]

[1]Department of Mechanics, Mathematics, and Management, Polytechnic University of Bari, 70126 Bari, Italy
[2]BionIT Laboratories, 73010 Soleto, Italy

Corresponding author: Giulio Reina (giulio.reina@poliba.it)

This work was supported in part by the Project giving Smell Sense To Agricultural Robotics (STAR), ERA-NET COFUND ICT AGRI-FOOD under Grant 45207; and in part by the Project NODES, which has received funding from the MUR-M4C2 1.5 of PNRR funded by the European Union-NextGenerationEU under Grant ECS00000036.

ABSTRACT The purpose of prosthetic hands is to replicate the functional capabilities of the human hand, allowing users to perform daily tasks effectively. The mechanical design of artificial fingers is a key factor in determining the overall performance of these prostheses. A novel solution in this field is the Adam Hand by BionIT Labs, which belongs to the family of underactuated, multiarticulated myoelectric prostheses. This paper presents a kinetostatic analysis of the Adam's Hand finger, which utilizes a gear train as an underactuated transmission mechanism. A test bench is also introduced to experimentally measure the grasping force when the finger spans its entire working range, defined by a 90° rotation of the proximal and distal phalanx joints. The experimental results demonstrate good agreement with the theoretical predictions, yielding mean percentage errors of less than 4%, with maximum error of about 6%. The analytical and experimental results obtained from Adam's hand are also compared with those of an alternative prosthesis, namely Bebionic, that is fully actuated.

INDEX TERMS Underactuated fingers, robotic hands, prosthetics, analytical modeling and analysis, experimental testing and validation.

I. INTRODUCTION

The human hand represents an exceptional and efficient system capable of executing intricate movements, ranging from strong to delicate tasks, perceiving and interacting with the environment. Therefore, upper limb amputation dramatically reduces the patient's autonomy and the capability of performing daily living, working, and social activities. Advances in technology have been aimed to improve the well-being of people with limb loss, as evidenced by the growing development of prosthetic hands in both the industrial and academic sectors. The period between 2010 and 2018 has seen a higher number of robotic hand designs compared to the entire previous century [1], [2]. Currently, there are four categories of prosthetic hands in use to restore different levels of functionality: cosmetic, body-powered, externally powered, and hybrid. Of these, extrinsically powered prosthetic hands represent the most promising solution to replicating human hand functionality due to their ability to intuitively provide all degrees of freedom (DoFs) of a human hand without any power input from the user [3]. However, their adoption has been limited due to high rejection rates that clearly indicate that not all user needs have been adequately addressed by modern externally powered prosthetic hands [4]. Most prostheses cannot achieve the recommended strength and speed capacity, and no one can achieve the anthropomorphic force and speed capacity while maintaining the anthropomorphic weight. Therefore, improvements in actuation and transmission remain important design challenges for future systems [5]. Notable examples of externally powered prostheses are: the Tactile sensor hand [6], I-Limb Quantum [7], VINCENTevolution3 [8], the Multigrasp Hand [9], Taska [10] and Bebionic [11]. In contrast to these fully actuated devices that tend to adopt

The associate editor coordinating the review of this manuscript and approving it for publication was Yangmin Li.

a similar number of actuated DoFs as the human hand, BionIT Labs has recently introduced Adam's Hand [12], shown in Fig. 1: a transradial myoelectric prosthesis based on the principle of underactuation, according to which a reduced number of actuators is designed to drive several degrees of freedom. In the case of Adam's Hand, 9 DOFs are controlled by two electric motors that is 2 degrees of actuation. This high degree of underactuation is achieved by stacking symmetrically three bevel gear differential stages, while the underactuation within each finger is obtained using gear trains. A more in-depth analysis of the proposed mechanism can be found in [12], [13].

This paper presents a theoretical kinetostatic analysis of the Adam Hand Finger that uses a gear train as the underactuated transmission mechanism. A test bed is also presented to experimentally assess the grasping force developed in different finger configurations, showing good agreement with the theoretical predictions. The analytical and experimental results obtained from Adam's Hand are also compared with those of the fully activated Bebionic prosthesis showing the differences between the two architectures. The theoretical and experimental comparison of an underactuated prosthetic finger with a fully actuated counterpart is seldom discussed in the literature and represents one of the novel contributions of the paper. Since the grasping force developed by the finger is strictly related with everyday use, it can be used as a performance metric that directly reflects the user's satisfaction. However, a standard benchmarking protocol to measure the finger force in prosthetic devices is missing in the literature with few examples devoted to industrial grippers only [14]. The other original contribution of this research is the proposal of an experimental protocol to quickly measure the force exerted by a prosthetic finger over all the working range of the finger rather than analyzing a single configuration (typically fully extended). In order to pursue these two research objectives, first, Sections II and III develop and analyze the kinematic and static modeling of the two prosthetic devices. Then, the theoretical results are experimentally validated using a dedicated test bed and protocol, as described in Section IV. Relevant conclusions are drawn in the final Section V.

II. ADAM'S HAND

The design of Adam's Hand inspires to the concept of underactuation that aims to design a mechanical system with a number of actuators lower than the degrees of freedom [16]. As described in the patent [17], the bevel gear differential transmission mechanism manages to distribute the power delivered by the drive motor - a palm-housed DC motor - to provide for the flexion/extension of the proximal and distal phalanges of the index, middle, ring and little fingers. As a result, the underactuated mechanism is qualified by what can be called "mechanical intelligence" [18], by virtue of which the actuation effort is equally distributed among the fingers and the passive adaptivity is achieved, i.e. when the motion of one or more fingers is prevented, the remaining finger(s) continue to move until a seamless adaptation to the grasped object is attained.

FIGURE 1. Adam's Hand: the underactuated prosthesis proposed by BionIT Labs [15].

A. KINETOSTATIC MODELING

The finger of Adam's Hand is shown in Fig. 2 along with its corresponding kinematic model. It is important to mention that unlike human hands, Adam's Hand has a proximal joint that resembles the human metacarpophalangeal joint (MCP) and a single distal joint that combines features of both the human proximal interphalangeal (PIP) and distal interphalangeal (DIP) joints [19]. Therefore, the finger has two phalanges: proximal and distal. Distal phalanx takes the form of both the middle and the distal one. Since the finger consists of two phalanges connected to each other and to the palm by two revolute joints, it has two degrees of freedom but only one actuation input, represented by the torque C_a in Fig. 2, making it an underactuated mechanism. The torque is transmitted to the phalanges through a gear train, with the final gear, which rotates around point C, fixed to the distal phalanx. When the proximal phalanx is stopped, the distal phalanx can continue to rotate until it contacts an object. Two elastic elements are placed at the MCP and PIP joints to produce a statically determined structure.

The static rotational equilibrium of the distal phalanx around the point C poses:

$$\boldsymbol{r}_{CG} \times \boldsymbol{F}_d + \boldsymbol{T}_d + \frac{R_2}{R_1}\boldsymbol{C}_a = 0 \tag{1}$$

where $\times$ indicates the vector product and (refer to Fig. 2):

$\boldsymbol{r}_{CG}$ denotes the position vector of the point G of application of the contact force with respect to C,
$\boldsymbol{F}_d$ is the external force applied to the distal phalanx,
$\boldsymbol{T}_d$ is the spring torque,
R_1 is the radius of the gear at the base of the proximal phalanx,
R_2 is the radius of the gear fixed to the distal phalanx,
$\boldsymbol{C}_a$ is the input torque provided by the actuation mechanism at the MCP joint.

By solving Eq. (1), the relationship between the magnitude of the actuation torque and that of the output force can be readily obtained:

$$F_d = \frac{T_d + (R_2/R_1)\, C_a}{k_d \cos\beta_d + \varepsilon_d \sin\beta_d} \tag{2}$$

where

k_d is the distance between the DIP joint and the contact point G,
β_d is the inclination angle of the force $\boldsymbol{F}_d$ relative to the perpendicular to the phalanx, as represented in Fig. 2,
ε_d is the thickness of the distal phalanx.

The magnitude of the spring torque, T_d, that appears in Eq.(2) depends on the stiffness and preload of the component and is, generally speaking, a function of the relative angle ϑ_d between the distal and the proximal phalanx.

III. BEBIONIC

Bebionic v2, shown in Fig. 3, is a multi-grip hand originally proposed by Steeper [20]. In the finger of Bebionic, the motion of the PIP is coupled with that of the MCP joint by means of a four-bar linkage that is marked in red in Fig. 4 for the index finger together with the corresponding kinematic model. Each finger is driven by a motor housed in the palm, allowing 14 different grip positions. The thumb has two phalanges as well. It has a passive abduction with two positions and its motor is housed in the finger structure itself. The knuckles are not aligned, but shaped as in a human hand in the rest configuration. The palm fingers can be manually closed via the pin slot joint E (refer to Fig. 4) to protect the mechanics of the hand.

A. KINETOSTATIC MODELING

As shown in Fig. 4, the Bebionic finger relies on a four-bar linkage mechanism to transmit the actuation force, F_a, to the two phalanges. The palm-housed drive motor is a custom linear drive that pulls the proximal phalanx at the rotational joint E via a nut screw mechanism (labeled H in Fig. 4). In this case, it is evident that the finger has only one degree of freedom, which means it is fully actuated. Consequently, the rotations of the two phalanges are rigidly coupled. In order to find out the kinematic relationship between the relative motion of the two phalanxes, a loop closure equation can be written as:

$$\boldsymbol{r}_{AB} + \boldsymbol{r}_{BC} + \boldsymbol{r}_{CD} + \boldsymbol{r}_{DA} = \boldsymbol{0} \tag{3}$$

where $\boldsymbol{r}$ is used to indicate the position vectors.

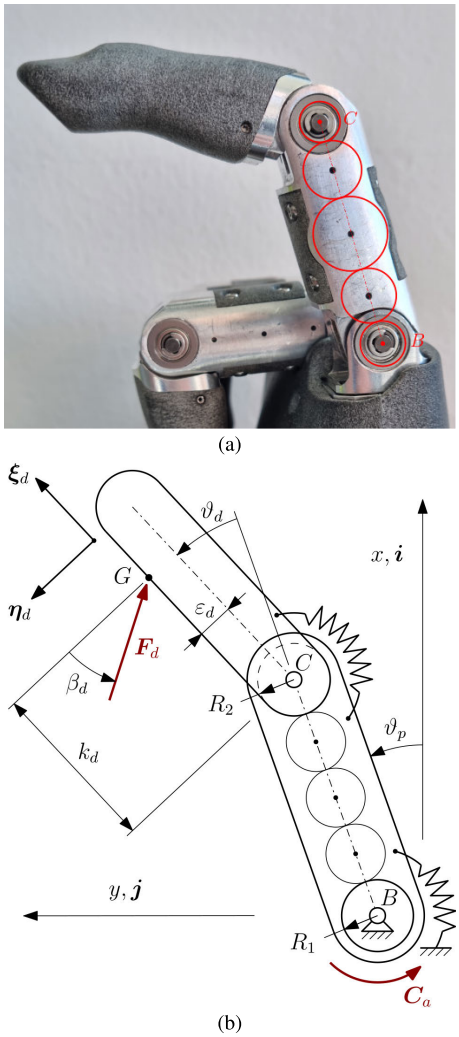

FIGURE 2. Kinematic model of finger joint coupling mechanism adopted by Adam's Hand: (a) original image, (b) kinematic scheme. The finger consists of the proximal and distal phalanges. The proximal phalanx is hinged to the palm at the metacarpophalangeal (MCP) joint, represented by point B. The distal phalanx is connected to the proximal phalanx by a revolute joint at point C, representing the proximal interphalangeal (PIP) joint. Both joints are equipped with springs, and the input torque, C_a, is transmitted to the phalanges via a gear train.

Squaring and adding the two scalar components of (3) yields:

$$L\cos(\vartheta_p + \vartheta_d) + M\sin(\vartheta_p + \vartheta_d) + N = 0 \tag{4}$$

where ϑ_p and ϑ_d are the angles associated with the rotation of the proximal and distal phalanx respectively (refer to Fig. 4), and

$$\begin{aligned} L &= 2l_{CD}\left(l_{AB}\cos\vartheta_{AB} + l_{BC}\cos\vartheta_p\right) \\ M &= 2l_{CD}\left(l_{AB}\sin\vartheta_{AB} + l_{BC}\sin\vartheta_p\right) \\ N &= l_{AB}^2 + l_{BC}^2 + l_{CD}^2 - l_{AD}^2 \\ &\quad + 2l_{AB}l_{BC}\left(\cos\vartheta_{AB}\cos\vartheta_p + \sin\vartheta_{AB}\sin\vartheta_p\right) \end{aligned}$$

in which the symbol l denotes the characteristic lengths of the finger linkage, and ϑ_{AB} represents the angle between the

FIGURE 3. Bebionic v2: the fully-actuated prosthesis proposed by Steeper [20].

x-axis and the vector $\boldsymbol{r}_{AB}$. In order to express the rotation of the distal phalanx as a function of the angle of the proposed phalanx, Eq. (4) can then be solved for the sum $(\vartheta_p + \vartheta_d)$ as follows:

$$\tan\left(\frac{\vartheta_p + \vartheta_d}{2}\right) = \frac{M \pm \sqrt{L^2 + M^2 - N^2}}{L - N}. \tag{5}$$

To calculate the contact force that the fingertip (point G in Fig. 4) can exert on an object as a function of the angle of the proximal phalanx, it is necessary to impose the static equilibrium of the two phalanxes, that gives:

$$\begin{cases} \boldsymbol{R}_B + \boldsymbol{R}_C + \boldsymbol{F}_a = \boldsymbol{0} \\ \boldsymbol{r}_{BE} \times \boldsymbol{F}_a + \boldsymbol{r}_{BC} \times \boldsymbol{R}_C + \boldsymbol{T}_d = 0 \\ \boldsymbol{R}_D - \boldsymbol{R}_C + \boldsymbol{F}_d = 0 \\ \boldsymbol{r}_{CD} \times \boldsymbol{R}_D + \boldsymbol{r}_{CG} \times \boldsymbol{F} - \boldsymbol{T}_d = 0 \end{cases} \tag{6}$$

where

- $\boldsymbol{R}_{\_}$ denotes the constraint reactions at the points specified as indices,
- $\boldsymbol{F}_a$ represents the actuation force, directed along the segment EH,
- $\boldsymbol{T}_d$ is the torque due to the spring located at the DIP joint,
- $\boldsymbol{F}_d$ is the force applied to the distal fingertip.

The first two rows in Eq. (6) refer to the balance of the proximal phalanx, the last two rows to that of the distal phalanx. The points chosen for moment calculation are the hinges B for the proximal phalanx and C for the distal one, so no torque contribution comes from $\boldsymbol{R}_B$ and $\boldsymbol{R}_C$ if the absence of friction is assumed. Solving Eq. (6), the desired relationship is found:

$$F_d = \frac{(a_1 + a_2)\, T_d + a_2 l_{BE} \cos\left(\vartheta_p + \alpha_p\right) F_a}{a_3 l_{CD} \sin\left(\vartheta_p + \vartheta_d - \psi\right) - a_1 l_{CG} \cos\left(\beta_d + \alpha_d\right)} \tag{7}$$

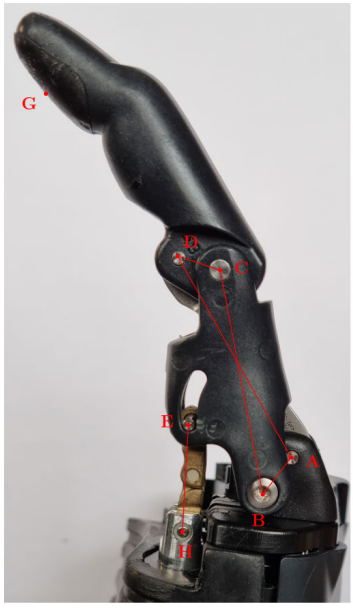

(a)

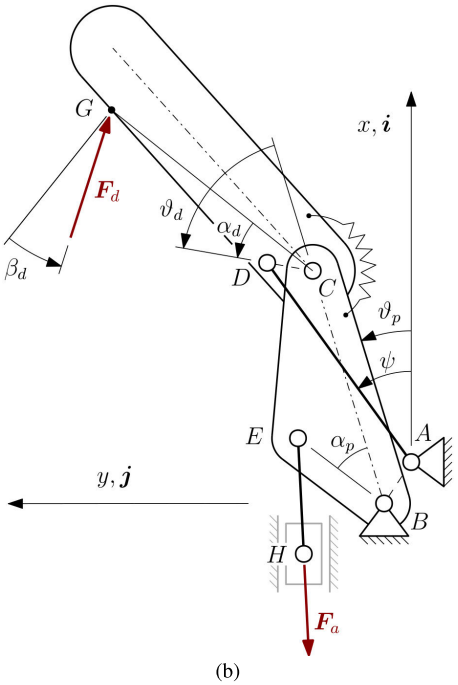

(b)

FIGURE 4. Bebionic index finger with overlaid the four-bar mechanism that couples the phalanx relative motion: (a) original image, (b) kinematic scheme. The finger is composed of the proximal and distal phalanges. The proximal phalanx is hinged to the palm at the metacarpophalangeal (MCP) joint, represented by point B. The distal phalanx is connected to the proximal phalanx by a revolute joint at point C, representing the proximal interphalangeal (PIP) joint. The latter is equipped with a spring. The actuation force, F_a, is transmitted to the phalanges through a four-bar linkage mechanism.

in which (refer to Fig. 4)

- α_p is the angle between the vectors $\boldsymbol{r}_{BE}$ and $\boldsymbol{r}_{BE}$,
- α_d is the angle between the vectors $\boldsymbol{r}_{CG}$ and $\boldsymbol{r}_{CD}$,
- ψ is the angle between the x-axis and the link AD,

and

$$a_1 = l_{BC}\sin(\vartheta_p - \psi)$$
$$a_2 = l_{CD}\sin(\vartheta_d + \vartheta_d - \psi)$$
$$a_3 = l_{BC}\cos(\vartheta_d + \beta_d)$$

IV. FINGER FORCE MEASUREMENT

The grasping force developed by the finger is directly related with the daily use of an upper limb prosthesis and is commonly adopted as a performance parameter as well as an indicator of user satisfaction. Despite its importance, the experimental procedures that researchers usually adopt to measure the force of the fingers are a one-off, which led to the recent effort to propose a standardized benchmarking protocol [14], [21], though mainly focused on robotic end-effectors and grippers rather than prosthetic devices. In this work, an experimental setup is arranged aimed to rapidly measure the force exerted by the single finger not only in a fully extended configuration but over all the working range of the finger itself. The tests performed are thoroughly described, together with the equipment and tools adopted, and the data obtained are compared with the numerical estimates derived from the models described in Section II and Section III for both hands involved in the current analysis.

A. EXPERIMENTAL TESTBED

The objective of the tests performed is to evaluate the force that prosthetic hands are capable of developing in the distal phalanges. To this end, the experimental testbed shown in Fig. 5 is set up. Among the main requirements for the test facility is the necessity to easily reposition the measuring device in order to accommodate different sizes and shapes of the analyzed hands, as well as spanning the entire range of motion of the fingers. To this end, aluminum extrusions assembled with removable corner brackets are used to realize the adjustable frame shown in Fig. 6.

The force is measured by means of the digital gauge SADFG-P0050 by SAMA Tools [22], featuring a resolution of 0.01 N, accuracy of $\pm$0.15 N, and minimum load equal to 0.1 N. It is mounted on a vertical upright that can be moved back and forth along the profile below (in the direction indicated as y-axis in Fig. 6); moreover, the measuring tool is constrained to the vertical beam through a 3D printed block that allows it to slide up and down (z-axis). Furthermore, the rotation of the measuring head about the x-axis is not constrained, but a revolute joint is arranged between the gauge and the upright to ensure an automatic repositioning of the tool due to the traction exerted by the finger during the test: this permitted rotation avoids the gauge to work in a tilted position with respect to the finger, thus undergoing unwanted lateral stresses which would be of no use given the uniaxial nature of the performed measurement. Such an adjustment would not be possible if the tests were conducted by letting the finger press on the probe, since the compression would give rise to unstable load configurations, thus necessarily requiring the repositioning and fixing of the meter each time. Another advantage of performing traction loading tests stems from the fact that it is remarkably easier to execute the measure over the entire range of motion of the finger (refer to Fig. 7), particularly when the sum of the angles of the phalanges, i.e. ϑ_p and ϑ_d in Fig. 2 and 4, exceeds 90°, as it would be impossible in that case to fit the gauge between the finger and the palm of the hand.

The prosthesis is fixed to the facility base by means of a metal plate with an embedded quick disconnect wrist (QDW). The QDW is used to firmly secure the prosthesis to the work table as it provides the very same electromechanical connection between the robotic hand and the prosthetic socket during normal use of the device [4]. Fixing the attachment plate using bolts allows to easily move the prosthesis along the x-axis of the frame (see Fig. 6), while the QDW allows to rotate the hand about the z-axis, in order for the testing probe to lie in the plane of motion of the finger. The prosthetic hands being tested are designed to be battery powered when they are worn by the user: since the force capability of such devices is strongly affected by the state of charge of the battery, the experimental campaign is carried out by using the laboratory power supply visible on the left in Fig. 5, at the nominal voltage of 7.4 V and current limitation equal to 10 A. The power supply parameters are chosen based on how the prosthetic hands are powered in their normal use. The battery systems supplied with both prostheses contain two lithium-ion cells, so the reference is set to the nominal voltage of 7.4 V, as declared by the manufacturers. The current limit is limited to 10 A, since the maximum continuous current of the aforementioned battery systems is lower than 6A [15], [20]. In a myoelectric prosthesis, the opening and closing commands are imparted, in most cases, by two electromyographic electrodes that convert the muscular contractions of the residual limb into 0-5 V signals read and interpreted by the prosthesis. The custom-made console emulates the signals provided by the electrodes, with one button deputed to the opening command and the other to the closing one. The output provided is a 0-5V step signal, through which the hand is controlled in on-off mode and can therefore be either at rest or exert the maximum force.

B. PROCEDURE

The following steps detail the procedure followed to conduct the experiment:

1) The hand is secured to the testbed using the QDW support. During this phase, particular care is taken to ensure that the tested finger (the index finger) lies in the same plane as the measuring probe, by adjusting the position of the wrist support along the x-axis.
2) The finger is positioned in a fully-extended configuration.
3) The vertical upright is positioned to align the measuring tool with the same z-coordinate as the chosen hooking point on the finger. The position along the y-axis is determined by the distance between the supporting bearing and the end of the pulling string.

FIGURE 5. Experimental testbed. On the left, the power supply is visible; on the right, the prosthetic hand is mounted on the test rig, with the index finger hooked to the measuring tool in the top-right corner. At the front, the two-button console used to issue the opening and closing signals for the finger is also shown.

FIGURE 6. Detailed view of the fixture system and measuring head. The supporting plate, which incorporates the quick-disconnect wrist (QDW) attachment for the prosthetic hand, can be moved along the *x*-axis. The vertical upright can slide along the *y*-axis, and the 3D-printed white block can be adjusted along the *z*-axis. This enables the precise repositioning of the measuring tool within the *y*-*z* plane relative to the finger.

4) The finger is commanded to close. This operation is performed using ON/OFF control, allowing the prosthesis to deliver maximum power.
5) After the string attached to the probe is tensioned, the pulling action exerted by the finger is maintained for a few seconds, then the finger is retracted to the starting position.
6) The measurement is repeated 30 times to achieve the desired sample size for the tested configuration.
7) The force is recorded throughout the test, and pictures of the finger in the loaded configuration are taken to estimate the angles of the phalanges and the direction of the force.
8) The measuring upright is moved to the following position, and the process is repeated starting from step 4.

Figure 8 illustrates an example of two repetitions of the force measurement (points 4 and 5 of the preceding list), along with the signals provided to the closing and opening electrodes used to drive the prostheses. The top plot shows the normalized force, calculated by dividing the measured force by the maximum value of force detected during the two cycles shown. The bottom plot shows the driving signals applied to the opening (blue) and closing (red) electrodes. After a 1-second long signal is applied to the opening electrode to retract the finger to the starting position, a similar 2-second signal is applied to the closing electrodes to flex the finger and exert force on the measuring probe. Then, for 5 seconds, both signals remain low before sending the open command for the next cycle.

The displacements of the measuring tool along the y and z axes, required to transition from one test configuration to the next (as outlined in point 8), are defined based on the knowledge of the working area derived from the kinematic analysis of the tested fingers. For each of the two hands tested, seven angles were chosen to balance the scope of the experimental campaign with the thoroughness of the analysis.

C. RESULTS AND DISCUSSION

The force values stated for prosthetic hands, especially commercial ones, are usually measured when the finger is in a fully open configuration [23]. In the present study, the fingers of both hands taken into account are characterized throughout their range of motion. This goal is achieved by fixing the prosthesis to the base plate and progressively moving the force gauge in discrete steps along a wide arc spanning all the state space $(\vartheta_p, \vartheta_d)$ of the finger, as illustrated in Fig. 7. The experimental result consists of two series, one for each analyzed hand, composed of seven different data sets corresponding to as many finger positions. For each test, the values of the angles adopted for the modeling of the finger architectures are deduced by superimposing digital goniometers onto high-resolution images, as shown in Fig. 9.

To numerically estimate the forces generated by the two prosthetic hands, in light of (2) and (7) it is necessary to know the actuation inputs C_a and F_a respectively, as well as the contributions T_d given by the springs. The latter are quantified by isolating the fingers of the two prostheses from their respective actuation mechanisms and progressively loading the joints to record the characteristic curves of the elastic elements. The collected data, consisting of deflection

FIGURE 7. Demonstrative sequence of traction tests for finger force measurement.

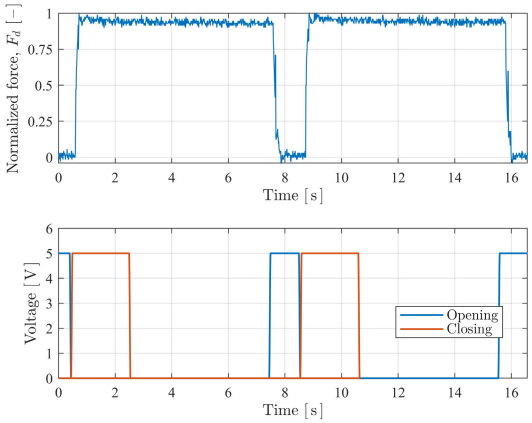

FIGURE 8. Example of fingertip force cycles: normalized force displayed at the top, and finger opening/closing signals shown at the bottom.

FIGURE 9. Extraction of the rotation angles of the proximal and distal phalanges from the high-resolution image of the finger.

angle-torque pairs, are fitted with quadratic polynomials to be fed into the relationships derived in Section II and III.

With regards to the generalized input forces C_a and F_a, specific tests are conducted to measure the performance of the actuation drivelines of the tested fingers, namely the torque applied to the gear at the base of the proximal phalanx in the case of Adam's Hand, and the pull force exerted on point E in Fig. 4 for Bebionic. In doing so, it is confirmed that the torque provided by the differential driveline of Adam's Hand does not vary significantly over all the range of rotation of the finger; similarly the actuation force of Bebionic is approximately constant along all the stroke of the plunger of the linear drive. Both the values of C_a and F_a are not disclosed to keep the information confidential. For the same reason, the forces plotted in Fig. 10 and 11, as well as those reported in Tables 1 and 2, are normalized by dividing them by the maximum values of the sample means recorded for Adam's Hand and Bebionic across all seven test configurations. The average values of repeated experimental tests (seven in our case) are shown as blue squares associated with bars representing the standard deviations of the data samples. The lines in red connect the force values predicted by the kinematic model for the same finger postures, i.e. calculated by replacing ϑ_p and ϑ_d in (2) and (7) with the angles of the phalanges detected during the tests. As evident from the graphs, the agreement between measured and predicted values is good, with mean errors of 4.00% for Adam's Hand and 3.59% for Bebionic. As reported in the last column of Tables 1 and 2, the percentage deviations, calculated from the difference between the mean values of the experimental samples and the predicted forces, are in all cases lower than 6% for Adam's Hand and 8% for Bebionic. These deviations are well below the maximum acceptable threshold of 10% for the analysis in question. Furthermore, as expected, both the experimental findings and the numerical evidence point out the different nature of the mechanisms adopted for the fingers of the two hands: while Bebionic is subject to a wider variation in force, Adam's Hand produces an approximately constant force output across the operating range. In other words, the transmission matrix is variable with the angle of the proximal phalanx for Bebionic, constant

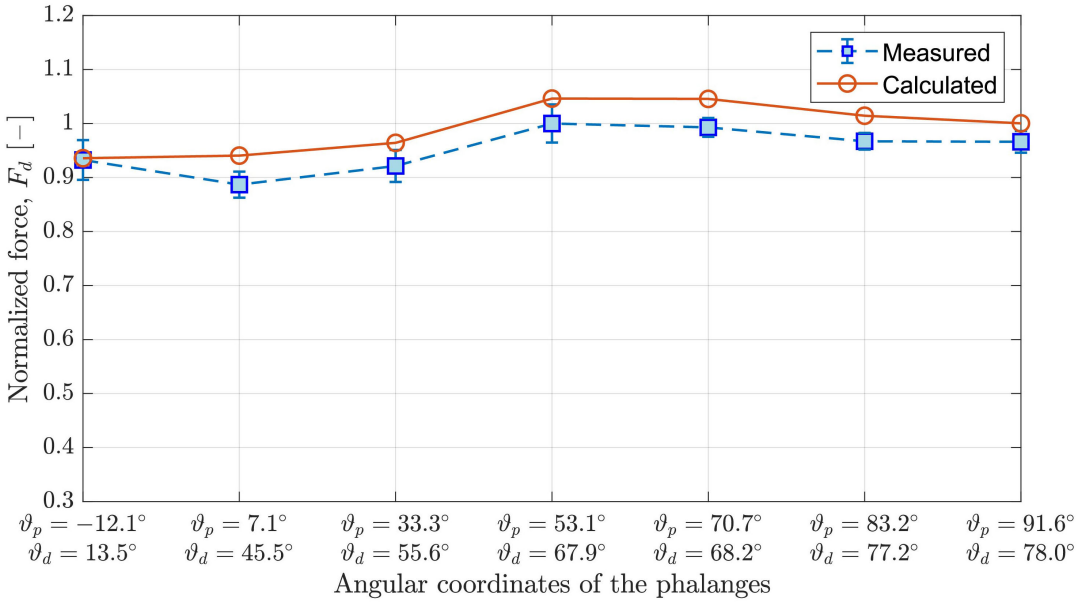

FIGURE 10. Comparison between measured and predicted normalized force for the finger of Adam's Hand.

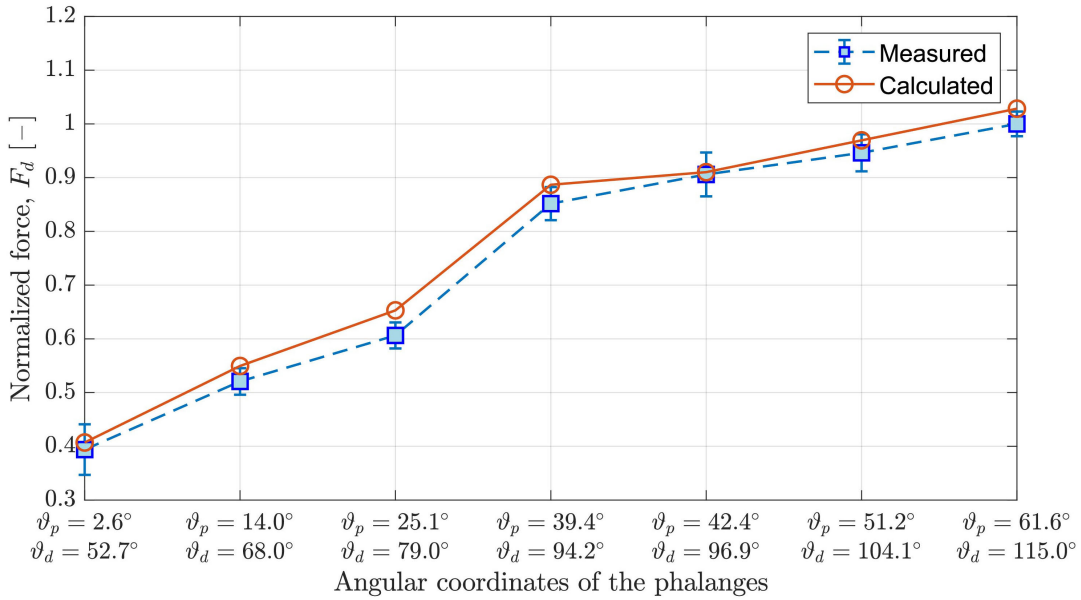

FIGURE 11. Comparison between measured and calculated normalized force for the finger of Bebionic.

for Adam's Hand. The latter, with its constant force profile throughout the range of motion, offers several advantages. A major benefit is the simplicity in user control. By delivering a predictable, steady force regardless of finger flexion, it reduces the cognitive load required from the user. This type of control is particularly helpful for users who perform repetitive tasks or need a consistent level of grip strength across various activities. Research supports the idea that reducing variability in the force profile can make prosthetic hands easier to control, especially for repetitive tasks that demand less fine-tuning in terms of force application. For example, a constant force allows users to focus on task execution rather than actively managing grip force [24], [25].

In contrast, Bebionic features a variable force profile, where force increases progressively as the fingers flex. This more closely mimics the behavior of the human hand, where greater force is exerted in more closed positions. This design, combined with the precisely predetermined trajectory of the phalanges, is more focused on the execution of pinch grasps and favors the precision manipulation tasks involving small objects. However, this comes at the cost of complexity, as more sophisticated control algorithms are required and users need to be more engaged in controlling the hand, which

may increase the cognitive load compared to a constant force system [26].

Based on the results obtained, it can be concluded that the analysis is fairly accurate in predicting the behaviour of the fingers of both hands in terms of force at the fingertip.

TABLE 1. Normalized fingertip force of Adam's Hand for each of the seven tested configurations: experimental sample mean (μ_{exp}), standard deviation (σ_{exp}), 95% confidence interval for the mean value (95% CI), theoretical prediction (F_d) and percentage deviation between F_d and μ_{exp} (%Δ).

Adam's Hand					
Test	μ_{exp}	σ_{exp}	95% CI	F_d	%Δ
T1	0.932	0.034	0.928 – 0.936	0.936	0.35
T2	0.887	0.021	0.884 – 0.889	0.941	5.71
T3	0.921	0.027	0.918 – 0.925	0.964	4.44
T4	1.000	0.035	0.996 – 1.004	1.046	4.42
T5	0.993	0.017	0.990 – 0.995	1.046	5.04
T6	0.967	0.015	0.965 – 0.969	1.014	4.66
T7	0.966	0.019	0.964 – 0.968	1.000	3.42

TABLE 2. Normalized fingertip force of Bebionic for each of the seven tested configuration: experimental sample mean (μ_{exp}), standard deviation (σ_{exp}), 95% confidence interval for the mean value (95% CI), theoretical prediction (F_d) and percentage deviation between F_d and μ_{exp} (%Δ).

Bebionic					
Test	μ_{exp}	σ_{exp}	95% CI	F_d	%Δ
T1	0.394	0.018	0.391 – 0.397	0.407	3.23
T2	0.521	0.013	0.519 – 0.522	0.549	5.23
T3	0.606	0.015	0.605 – 0.608	0.653	7.14
T4	0.852	0.026	0.849 – 0.855	0.887	3.96
T5	0.906	0.037	0.902 – 0.909	0.910	0.47
T6	0.946	0.033	0.942 – 0.950	0.969	2.39
T7	1.000	0.023	0.997 – 1.002	1.028	2.75

V. CONCLUSION AND FUTURE DEVELOPMENTS

In this paper, two externally powered prosthetic hands, namely Adam's Hand and Bebionic, were analyzed, focusing on the mechanical characteristics and performance of the fingers. For both architectures, relationships were derived that give the force at the fingertip as a function of actuation input, spring torque, as well as geometric parameters. The numerical results were compared with the measurements of the finger force taken using a dedicated test bed that was designed aiming to simplicity and flexibility. Those requirements are dictated by the intention to end up with a test facility at the same time cost-effective and suitable for end-of-line quality control of such devices like the upper limb prostheses. Future research will be focused on refining the analysis proposed here by introducing loss terms and inertial effects, as well as improving the test bed as for ease of use and speed of execution of the experimental campaign.

REFERENCES

[1] C. Piazza, G. Grioli, M. G. Catalano, and A. Bicchi, "A century of robotic hands," *Annu. Rev. Control, Robot., Auto. Syst.*, vol. 2, no. 1, pp. 1–32, May 2019.
[2] E. Difonzo, G. Zappatore, G. Mantriota, and G. Reina, "Advances in finger and partial hand prosthetic mechanisms," *Robotics*, vol. 9, no. 4, p. 80, Oct. 2020.
[3] R. Damerla, Y. Qiu, T. M. Sun, and S. Awtar, "A review of the performance of extrinsically powered prosthetic hands," *IEEE Trans. Med. Robot. Bionics*, vol. 3, no. 3, pp. 640–660, Aug. 2021.
[4] D. C. Potenza, A. Grazioso, F. Gaetani, G. Mantriota, and G. Reina, "A smart demonstration unit for upper-limb myoelectric prostheses," *Smart Health*, vol. 32, Jun. 2024, Art. no. 100481.
[5] J. T. Belter, J. L. Segil, A. M. Dollar, and R. F. Weir, "Mechanical design and performance specifications of anthropomorphic prosthetic hands: A review," *J. Rehabil. Res. Develop.*, vol. 50, no. 5, p. 599, 2013.
[6] T. Zhang, L. Jiang, and H. Liu, "Design and functional evaluation of a dexterous myoelectric hand prosthesis with biomimetic tactile sensor," *IEEE Trans. Neural Syst. Rehabil. Eng.*, vol. 26, no. 7, pp. 1391–1399, Jul. 2018.
[7] Össur, Reykjavík, Iceland. *I-Limb Quantum Catalog*. Accessed: Oct. 11, 2024. [Online]. Available: https://www.ossur.com/en-us/prosthetics/arms/i-limb-quantum?tab=specification
[8] S. Hussain, S. Shams, and S. J. Khan, "Impact of medical advancement: Prostheses," in *Computer Architecture in Industrial, Biomechanical and Biomedical Engineering*. IntechOpen, 2019.
[9] D. A. Bennett, S. A. Dalley, D. Truex, and M. Goldfarb, "A multi-grasp hand prosthesis for providing precision and conformal grasps," *IEEE/ASME Trans. Mechatronics*, vol. 20, no. 4, pp. 1697–1704, Aug. 2015.
[10] TASKA Prosthetics, Christchurch, New Zealand. *TASKA Hand Specification Sheet*. Accessed: Oct. 11, 2024. [Online]. Available: https://www.taskaprosthetics.com/support
[11] C. Widehammar, A. Hiyoshi, K. Lidström Holmqvist, H. Lindner, and L. Hermansson, "Effect of multi-grip myoelectric prosthetic hands on daily activities, pain-related disability and prosthesis use compared with single-grip myoelectric prostheses: A single-case study," *J. Rehabil. Med.*, vol. 54, Nov. 2021, Art. no. 100481.
[12] G. Zappatore, G. Reina, and A. Messina, "Analysis of a highly underactuated robotic hand," *Int. J. Mech. Control*, vol. 18, no. 4, pp. 17–23, 2017.
[13] A. Grazioso, C. Danese, G. A. Zappatore, and G. Reina, "A multibody approach for the finger force estimation of a robotic hand," in *Biomimetic and Biohybrid Systems*, F. Meder, A. Hunt, L. Margheri, A. Mura, and B. Mazzolai, Eds., Cham, Switzerland: Springer, 2023, pp. 70–83.
[14] J. Falco, D. Hemphill, K. Kimble, E. Messina, A. Norton, R. Ropelato, and H. Yanco, "Benchmarking protocols for evaluating grasp strength, grasp cycle time, finger strength, and finger repeatability of robot end-effectors," *IEEE Robot. Autom. Lett.*, vol. 5, no. 2, pp. 644–651, Apr. 2020.
[15] *Bionit Labs*. Accessed: Oct. 11, 2024. [Online]. Available: https://bionitlabs.com/
[16] L. Birglen, T. Laliberté, and C. Gosselin, "Design and control of the Laval underactuated hands," in *Underactuated Robotic Hands*. Cham, Switzerland: Springer, 2007, pp. 171–207.
[17] G. Zappatore, M. Dimastrogiovanni, A. Longo, D. Tinella, and A. Accogli, "Mano robotica sottoattuata," IT Patent 202 200 012 392 A1, Dec. 13, 2023.
[18] C. M. Gosselin, L. Birglen, and T. Laliberté, *Underactuated Robotic Hands*. Berlin, Germany: Springer, 2007.
[19] *Joints*. Accessed: Oct. 11, 2024. [Online]. Available: https://www.assh.org/handcare/safety/joints
[20] *Steeper Prosthetics*. Accessed: Oct. 11, 2024. [Online]. Available: https://www.steepergroup.com/prosthetics/
[21] J. A. Falco, K. Van Wyk, and E. R. Messina, "Performance metrics and test methods for robotic hands (draft)," NIST Nat. Inst. Standard Technol., US Dept. Commerce, Tech. Rep. 1227, Oct. 31, 2018.
[22] SAMA, Viareggio, Italy. *High Precision Digital Force Gauges*. Accessed: Oct. 11, 2024. [Online]. Available: https://samatoolsgroup.com/en/prodotto/high-precision-digital-force-gauges-sadfg-p/
[23] U. Wijk, A. Björkman, I. K. Carlsson, F. Kristiansdottir, A. Mrkonjic, B. Rosén, and C. Antfolk, "A bionic hand versus a replanted hand," *J. Rehabil. Med.-Clin. Commun.*, vol. 7, p. 24854, Jan. 2024.
[24] N. Malesevic, A. Björkman, G. S. Andersson, C. Cipriani, and C. Antfolk, "Evaluation of simple algorithms for proportional control of prosthetic hands using intramuscular electromyography," *Sensors*, vol. 22, no. 13, p. 5054, Jul. 2022.
[25] C. Gentile, F. Cordella, and L. Zollo, "Hierarchical human-inspired control strategies for prosthetic hands," *Sensors*, vol. 22, no. 7, p. 2521, Mar. 2022.
[26] Q. Fu and M. Santello, "Learning from the human hand: Force control and perception using a soft-synergy prosthetic hand and noninvasive haptic feedback," in *Advances in Motor Neuroprostheses*. Cham, Switzerland: Springer, 2020.

ANDREA GRAZIOSO was born in Gallipoli, Italy, in 1989. He received the B.S. degree in industrial engineering and the M.S. degree in mechanical engineering from the University of Salento, Lecce, in 2013 and 2021, respectively. He is currently pursuing the Ph.D. degree with the Department of Mechanics, Mathematics, and Management, Polytechnic University of Bari, Italy, where his research is co-funded by BionIT Laboratories. From 2022 to 2023, he was a Research Fellow with the Robotic Mobility Laboratory, Polytechnic University of Bari, where he worked on the multibody modeling and simulation of autonomous tracked vehicles. His current research interests include sensor integration, biomimetic design, and haptic feedback in prosthetics.

DAMIANO COSMA POTENZA received the B.S. degree in physics and the M.S. degree in matter physics from the University of Salento, Lecce, in 2013 and 2015, respectively. He is currently pursuing the Ph.D. degree with the Department of Mechanics, Mathematics, and Management, Polytechnic University of Bari, Italy, where his research is co-funded by BionIT Laboratories. From 2016 to 2020, he was involved in firmware validation and fire hazard tests in automotive HVAC systems in Turin, Italy. During the same period, he designed and developed the software and hardware for an end-of-line system to check HVAC control units. His research is the development of an innovative EMG acquisition systems.

GIOVANNI ANTONIO ZAPPATORE was born in Maglie, Italy, in 1991. He received the B.S. degree in industrial engineering and the M.S. degree in mechanical engineering from the University of Salento, in 2014 and 2017, respectively. In 2018, he founded BionIT Laboratories, a Medtech Italian company operating in the fields of bionics and human–machine integration, of which today he is the CEO and President. His current research interests include the design and development of biomimetic prostheses and underactuated mechanisms.

GIULIO REINA received the Laurea and the Research Doctorate degrees in mechanical engineering from Polytechnic University of Bari, Italy, in 2000 and 2004, respectively. From 2002 to 2003, he was with the Mobile Robotics Laboratory, University of Michigan, as a Visiting Scholar. In 2010, he was also selected to receive an Endeavour Research Fellowship with the Australian Centre for Field Robotics, The University of Sydney. Currently, he is a Full Professor with the Department of Mechanics, Mathematics, and Management, Polytechnic University of Bari. His research interests include mobile robotics for agriculture and planetary exploration, vehicle dynamic modeling and estimation, and underactuated grasping systems. In 2007, he was awarded a Japanese Society for Promotion of Science (JSPS) Fellowship for a one-year research with the Space Robotics Laboratory, Tohoku University, Sendai, Japan.

Open Access funding provided by 'Politecnico di Bari' within the CRUI CARE Agreement